SUMMARY OF FINITE ELEMENT (FE) SENSITIVITY STUDIES CONDUCTED IN SUPPORT OF THE NRC/EPRI WELDING RESIDUAL STRESS (WRS) PROGRAM

Matthew Kerr and Howard J. Rathbun[†],[‡]
Office of Nuclear Regulatory Research
U.S. Nuclear Regulatory Commission
Washington, DC 20555

ABSTRACT

The U.S. Nuclear Regulatory Commission (NRC) and the Electric Power Research Institute (EPRI) are working cooperatively under an addendum to the ongoing memorandum of understanding to validate welding residual stress (WRS) predictions in pressurized water reactor (PWR) primary cooling loop components containing dissimilar metal (DM) welds. These stresses are of interest as DM welds in PWRs are susceptible to primary water stress corrosion cracking (PWSCC) and tensile weld residual stresses are the primary driver of this degradation mechanism. The NRC/EPRI weld residual stress (WRS) analysis validation program consists of four phases, with each phase increasing in complexity from laboratory size specimens to component mock-ups and ex-plant material.

This paper focuses on Phase 2 of the WRS program that included an international Finite Element (FE) WRS round robin and experimental residuals stress measurements using the Deep Hole Drill (DHD) method on pressurizer surge nozzle mock-up. Characterizing variability in the round robin data set is difficult, as there is significant scatter in the data set and the WRS profile is dependent on the form of the material hardening law assumed. The results of this study show that, on average, analysts can develop WRS predictions that are a reasonable estimate for actual configurations as quantified by measurements. Sensitivity studies assist in determining which input parameters provide significant impact on WRSs, with thermal energy input, post-yield stress-strain behavior, and treatment of strain hardening have the greatest impact on DM WRS distributions.

INTRODUCTION

In pressurized-water reactor (PWR) coolant systems, nickel based Dissimilar Metal (DM) welds are typically used to join carbon steel components, including the reactor pressure vessel, steam generators, and the pressurizer, to stainless steel piping. Figure 1 shows a cross-section of a representative nozzle to piping connection, including the DM weld [1,2]. In Figure 1, the DM weld is indicated as "Alloy 82/182 Butt Weld." The DM weld is fabricated by sequentially depositing weld passes as high-temperature molten metal that cools, solidifies, and contracts, retaining stresses that approach or, potentially, exceed the material's yield strength.
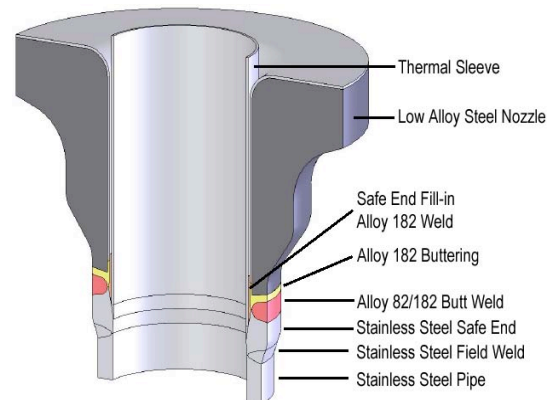

Figure 1 Representative Nozzle Cross Section.

These DM welds are susceptible to primary water stress-corrosion cracking (PWSCC) as an active degradation mechanism that has led to reactor cooling system pressure boundary leakage. Within a DM weld in a corrosive environment, PWSCC is driven by tensile weld residual

[†] Corresponding author, howard.rathbun@nrc.gov
[‡] The views expressed herein are those of the authors and do not represent an official position of the US Nuclear Regulatory Commission.

stresses (WRS) and other applied loads. Hence, proper assessment of these stresses is essential to accurately predict PWSCC flaw initiation, growth and stability.

Recent improvements in computational efficiency have facilitated advances in WRS predictions, but no universally accepted guidelines for these analyses have been established. Therefore, the assumptions and estimation techniques employed vary from analyst to analyst, causing large variability in the predicted residual stress profiles for a given weld.

The U.S. Nuclear Regulatory Commission (NRC) staff and its contractors are completing a WRS analysis validation program aimed at both (1) refining computational procedures for residual stress simulations in DM welds, and (2) developing and categorizing the uncertainties in the resulting residual stress predictions. This program consists of four phases, with each phase increasing in complexity [3-5]. Parts of this program are being cooperatively completed with the Electric Power Research Institute (EPRI) under an addendum to the ongoing Memorandum of Understanding (MOU). [6]

The second phase of this program consists of an analytical international round-robin for validation of predicted WRSs in a prototypical PWR pressurizer surge nozzle geometry. The results from the round robin are to be validated through comparison of predicted residual stress fields with a variety of physical measurements performed on the mock-up. The validation is double blind, i.e., the FE analysis and measurement participants are not allowed to compare their results before submission, permitting the NRC staff to develop unbiased measures of uncertainties in WRS predictions.

The NRC staff's objectives in completing this research program include:

- Support the NRC's Office of Nuclear Reactor Regulation (NRR) development of appropriate WRS/flaw evaluation review guidelines.
- Perform independent confirmatory research on industry guidance for performing WRS analysis.
- Assess and evaluate the near-term adequacy of industry's mitigation activities where WRS minimization is necessary.
- Improve WRS finite element analysis (FEA) predictive methodologies.
- Assess variability of WRS (mean and distribution).
- Determine estimates for the uncertainty and distribution of WRS, which are needed in probabilistic analyses (e.g., xLPR Code – eXtremely Low Probability of Rupture [7]).

PHASE 2 MOCK-UP

The geometry chosen for the WRS round robin is representative of a pressurizer surge nozzle, due to its safety significance and relevance to flaw evaluation [8,9]. The overall geometry is shown in Figure 1. For this mock-up, the nozzle (SA-105 nozzle from a cancelled reactor) is buttered with Alloy 82 (AWS A5.14, ERNiCr-3, UNS N06082) weld material, post weld heat treated and then welded to a forged F316L stainless steel safe-end. Finally, the safe-end is welded to a TP316 stainless steel, 14-inch diameter Schedule 160 stainless steel pipe using a TP308 weld.

The mock-up is fabricated in the following four steps. The carbon steel nozzle is buttered with 137 passes of Alloy 82. After heat treating and machining the butter, 40 passes of Alloy 82 are deposited to make up the main DM weld. The root of the main weld is then machined and 27 passes deposited with Alloy 82 to make up the 360 degree fill-in weld. At this point, residual stress measurements are made on the DM welds. The residual stress measurements are followed by the TP308 stainless steel safe-end to pipe weld, with a second set of residual stress measurements made investigating the effect of the safe-end to pipe weld. For the main DM weld and fill-in weld, laser profilometry measurements are made to map the contour of each weld pass.

FINITE ELEMENT RESULTS AND EXPERIMENTAL MEASUREMENTS

For the results summarized in this paper and plotted in Figure 2, analysts were provided bead geometry (laser profilometry), thermocouple, and material property data. In all cases there is general agreement in terms of the WRS profile shape and the DHD data, visualized by the comparison of the FE averages to the DHD measurements. Two averages are plotted, the average of FE results using (1) isotropic and (2) kinematic hardening as this effects the form of the WRS profile. In general there is better agreement between the isotropic average, in terms of profile shape and stress magnitude, though this is not the case for all locations through thickness. Further while there is general agreement between the isotropic average stresses calculated by FE and the DHD measurements, there is not consistency between the stress magnitudes calculated by the FE and the DHD measurements (i.e. the DHD results are not always high with respect to the FE results).

Variability in the FE results is discussed in greater detail in the next section, but is approximately ±200 to 250 MPa for axial and hoop stresses both before and after application of the safe-end weld. The variability in the FE results is significantly greater than the observed variability in the DHD measurements. Prior to the safe-end weld there are results for two DHD measurements, while similar in WRS profile and stress magnitude it is difficult to comment on the repeatability of such a small dataset. After application of the safe-end weld there are results for a total of 6 DHD results, exhibiting an apparent variability within ±50 MPa through thickness. While this dataset of DHD measurements post safe-end weld are still small, the addition measurements build confidence in the

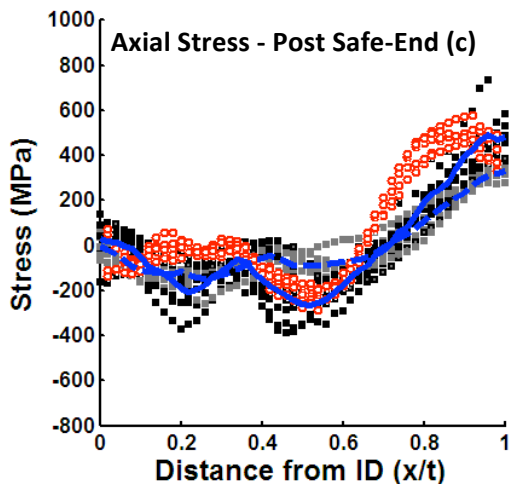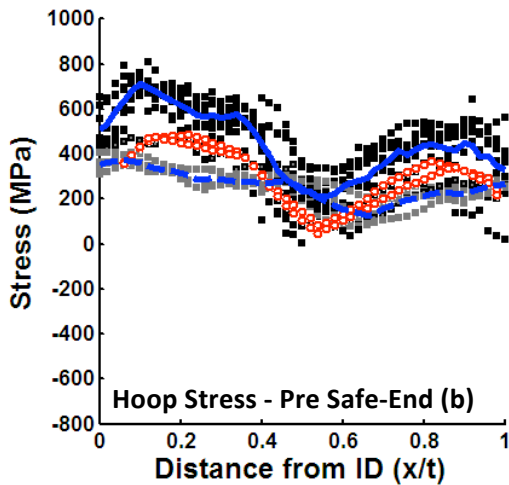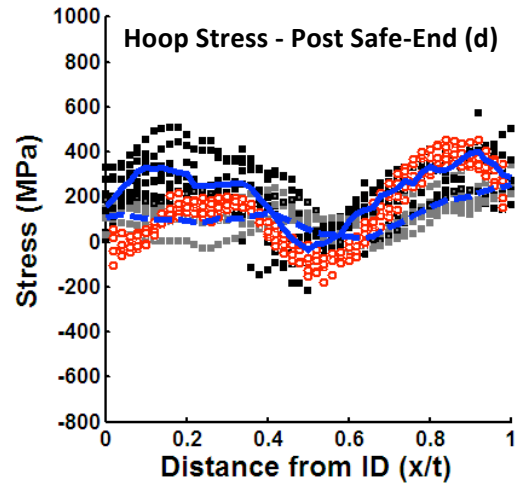repeatability of the DHD measurements conducted in support of the Phase 2 effort.
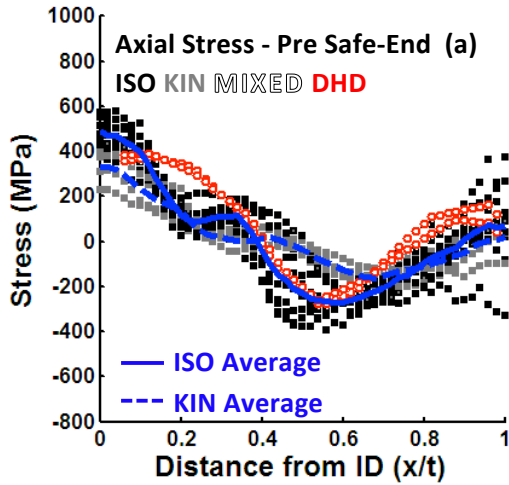

Figure 2 Summary of FE WRS results and experimental DHD measurements from Phase 2 of the NRC/EPRI WRS Program, (a, b) pre safe-end weld and (c, d) post safe-end weld WRS distributions.

ROUND ROBIN DATASET VARIABLITY

Finite Variability in the round robin dataset is significant and difficult to characterize, as the calculated WRS profile is dependent on the form of the hardening law assumed. Variability in the section is presented using three methods of classification (1) calculating the standard deviation for the entire dataset, including all FE results, (2) the min/max values of the entire round robin dataset, and (3) the min/max values of a subset of the round robin dataset, specifically results from US nuclear industry and NRC contractors. At each of the 50 points through thickness, the average and standard deviation (σ) of all FE results is calculated as,

$$\sigma = \sqrt{\frac{1}{N-1} \sum_{i=1}^{N}(x_i - \bar{x}_i)^2}$$

where N is the number of data sets, x is the value (stress), and $\overline{x}$ is the average value (average stress). All of the FE results and DHD measurements were included in the averages, due to the limited size of the round robin dataset. The use of standard deviation as a repression of variability assumes that the dataset is normally distributed. The dataset was tested for uniformity, but could not be tested for normality due to the small sample size. Min and max values of the dataset were also recorded at each of the 50 points through thickness.

For the axial and hoop stresses, there is good agreement between ±2 standard deviations of the entire dataset and the

min/max values of all FE results before (Figure 3) and after application of the safe-end weld (Figure 4). As the WRS profile is dependent on the form of the hardening law assumed, a subset of the in/max isotropic results, consisting of the isotropic results from US nuclear industry and NRC contractors, are plotted against the ±2 standard deviations for the entire round robin dataset. Standard deviations are not calculated for this subset of results as the sample size is quite small, 6 results versus 15 for the entire round dataset.

Axial stresses prior to the safe-end weld are plotted in Figure 3 (a, b). The smallest reduction in variability is between 0.3 to 0.5 x/t where the stress first crosses zero and is consistent with the observation that, for isotropic models, the location where the axial stress first crosses zero is sensitive to heat input. A similar reduction in variability is observed in axial stress after application of the safe-end weld plotted in Figure 3 (a, b), but only for x/t greater than 0.5. Prior to x/t of 0.5, the axial variability for this subset of the round robin dataset remains essentially unchanged. Hoop WRS profiles before and after application of the safe-end weld are plotted in Figure 3 (c, d) and Figure 4 (c, d), respectively. Min/max values for the hoop stresses tend to shift towards the +2 sigma bound of the entire round robin, as for the hoop stresses the isotropic results are higher in stress than the kinematic results.
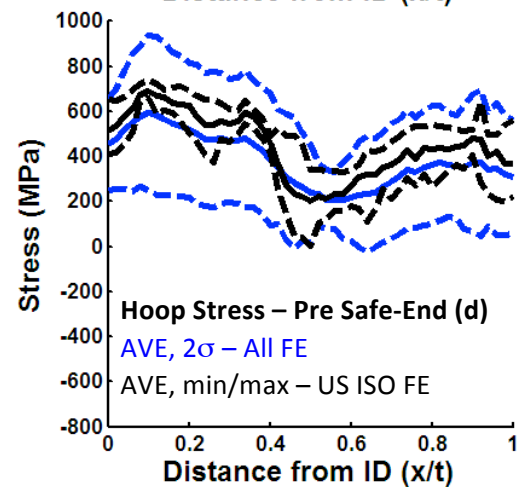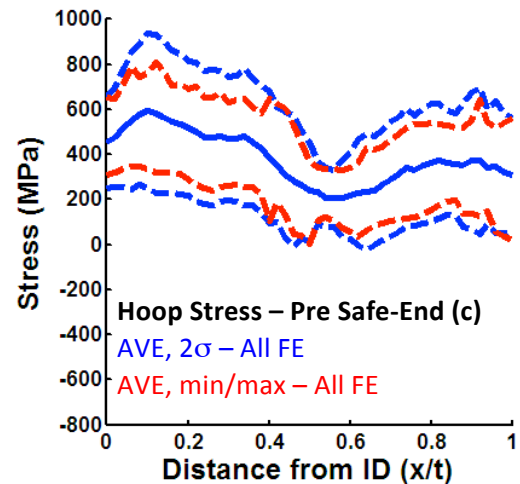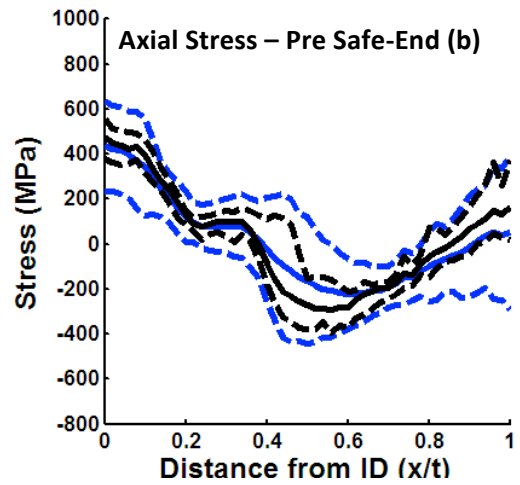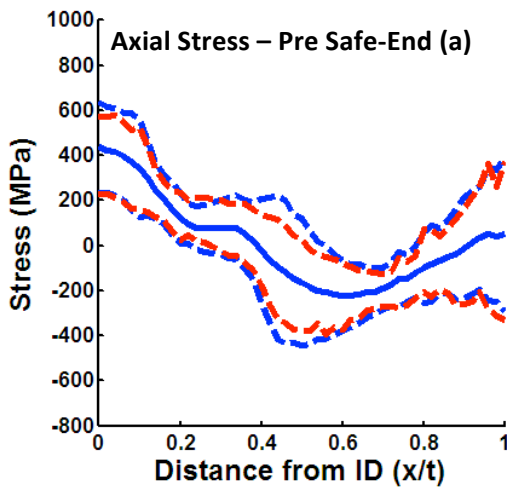

Figure 3 Comparison Phase 2 dataset variability pre safe-end weld, in general there is good agreement between the 2σ of the entire dataset and the min/max values of all the FE results (a, c). Min/max values of the US isotropic results exhibit lower variability than the 2σ of the entire dataset (b, d).
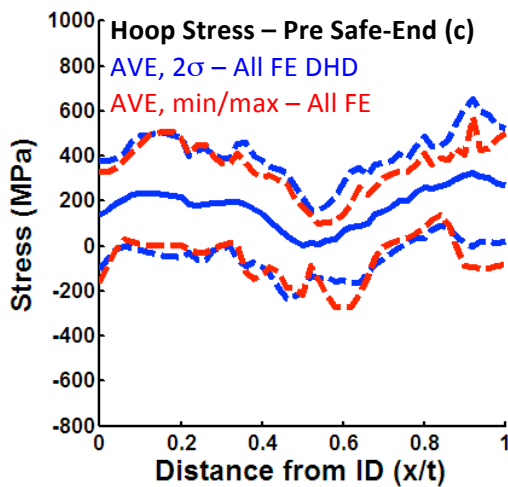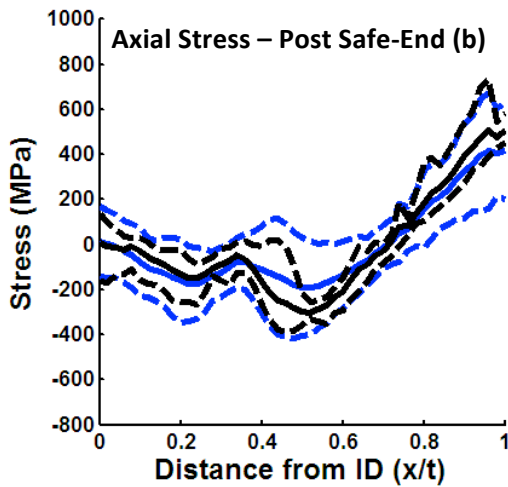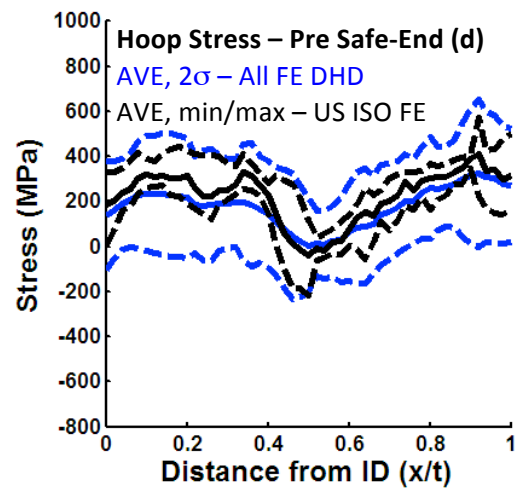
Figure 4 Comparison Phase 2 dataset variability pre safe-end weld, in general there is good agreement between the 2σ of the entire dataset and the min/max values of all the FE results (a, c). Min/max values of the US isotropic results exhibit lower variability than the 2σ of the entire dataset (b, d).
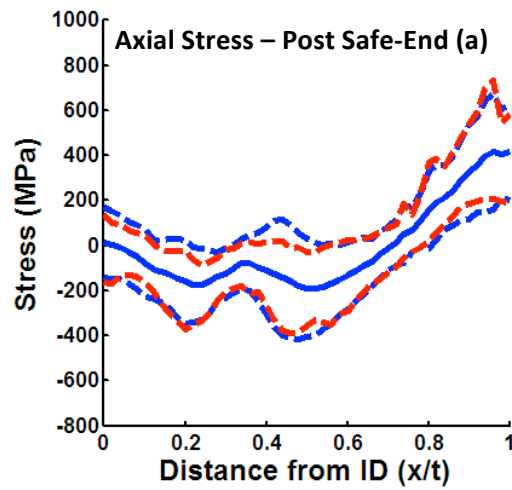
SENSITIVITY STUDIES

Given the presentation and analysis of the previous section, it is apparent that significant variation exists in the round robin FE data sets. In practice, this high degree of scatter inherently reduces confidence that FE calculation results are reasonable approximations to the true, physical state of stress of a structure. WRS FE simulations are complex in that there are many input variables and methods for approximating model details. Further, WRS fields are known to have a significant effect on flaw evaluation and probabilistic fracture mechanics calculation results. Therefore, it is important to gain an understanding of the significant sources of variability in WRS FE calculations. As a corollary, it is also useful to understand which FE input parameters have negligible effects on results, to avoid unnecessarily expending resources on model aspects that have little to no bearing on final results.

The standard procedure for assessing the impact of individual FE model inputs and features is to systematically vary individual parameters, run the analysis and determine the effect on the results. In the current study, the following procedure is employed:

1. Develop a FE model that is validated with respect to other FE results and measurements
2. Identify the full set of possible model inputs and features that are likely to have a significant impact on final results

3. Systematically vary the remaining model input parameters and features; observe and quantify the results

The following sections describe the above procedure as applied to the round robin nozzle study.

Baseline Model Development and Validation

A model is generated as a basis for comparison in the sensitivity studies. Important model development aspects are described, including geometry, thermal analysis, mechanical analysis and model validation. The model is developed and run in the commercially available finite element code ABAQUS [15]. For simplicity and to facilitate direct comparison with round robin participant results, the model is two-dimensional axi-symmetric. The thermal and structural portions of the analysis are de-coupled. The time duration at which weld-deposited material exists at high temperature is relatively short; hence, creep behavior is not addressed in this analysis.
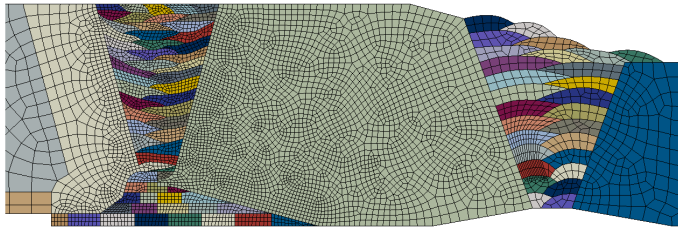

Figure 5 Close-up of DM and stainless steel weld meshes and surrounding materials.

Model Inputs and Features

The input categories can be consolidated into the following groupings:

- Thermal
- Energy magnitude and duration (dictated by weld voltage, current, arc efficiency and deposition speed)
- Density
- Latent heat
- Conductivity
- Specific heat
- Convective heat transfer coefficient
- Mechanical
- Coefficient of thermal expansion
- Elastic properties (modulus and Poisson ratio)
- Plastic properties (true stress vs. plastic strain)
- Hardening law
- Anneal temperature
- Weld bead shape
- Weld pass order of deposition

Experience has shown that, within the range of reasonable values that an experienced analyst would choose, variations in several of these parameters have negligible effects on final analysis results. For example, material density is a parameter required to perform the thermal analysis portion. Minor variations in readily available (e.g. handbook) density values for the materials of interest are known from experience to yield little to no difference in final results. Hence, there is no need to perform sensitivity studies involving density.

Following this logic, the remaining parameters of interest that are considered in the current study include energy magnitude and duration, coefficient of thermal expansion, elastic modulus, plastic properties (true stress vs. plastic strain), hardening law (isotropic and kinematic), anneal temperature, and weld pass order of deposition. The following sections describe systematic variation of these model parameters and aspects, and their impact on centerline through-wall DM weld axial and hoop stresses. It is found that some of these model parameters have a significant effect on weld residual stresses, and some have a negligible effect.

In several of these studies, three representative sets of material properties are referred to, one employed by Engineering Mechanics Corporation of Columbus (EMC2) in participating in a British Energy (BE) lead WRS validation effort [20] referred to as "BE properties", the second set of properties were distributed to round robin participants referred to as "Phase 2 properties", and a third set of properties from previous EMCC and NRC studies that was used in the current baseline model referred to as "Baseline properties".

Heat Flux Magnitude and Duration

Intuitively, the magnitude and duration of heat flux input during the welding simulation would have an effect on final through-wall stress distributions. To quantify these effects, independent sensitivity studies are performed in which the magnitude and duration of weld heat flux are varied relative to the baseline analysis. The thermal model described in [16] provides a convenient means of independently varying weld heat flux magnitude and duration; by varying input parameters in this model, a range of heat flux magnitudes and durations can be achieved.

The magnitude of heat flux varies linearly with arc efficiency. In this study, the baseline arc efficiency values are scaled by factors of 0.25, 0.5 and 1.5 to provide a wide range of heat flux values. Note that only the arc efficiencies of the DM weld are scaled, whereas the arc efficiencies of the stainless steel weld remain unchanged. Figure 6 shows the resulting heat flux magnitudes as a function of time, including the baseline case. In completing the weld heat flux magnitude sensitivity study, both the thermal analysis and structural analysis must be performed. Figures 7 and 8 show the final through-wall centerline DM weld axial and hoop stress distributions, before and after application of the stainless steel

weld, for the various heat flux magnitude inputs. Clearly, for the magnitude of heat flux variation chosen, significant differences in final through-wall stresses is observed.
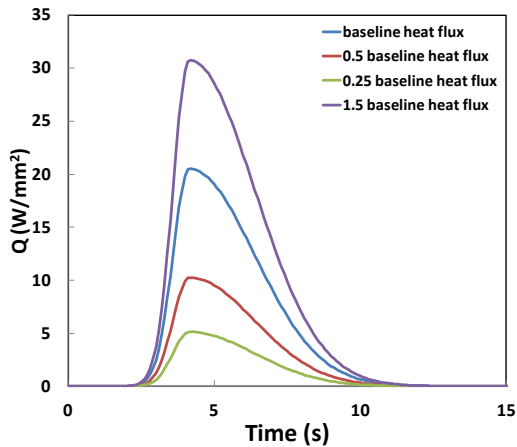

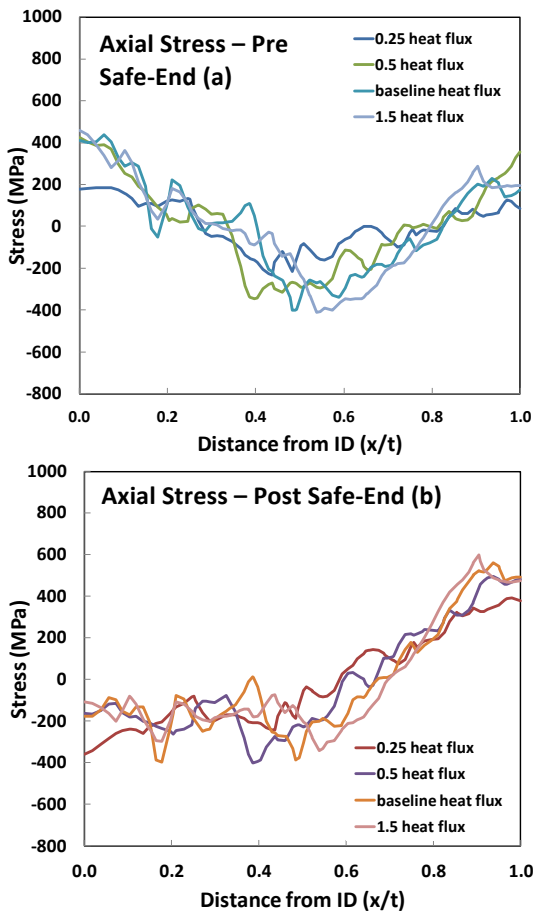**Figure 6** Heat flux vs. time for magnitude sensitivity study.

Figure 7 Axial stress results for heat flux magnitude sensitivity study (a) pre- and (b) post-stainless steel safe-end weld.
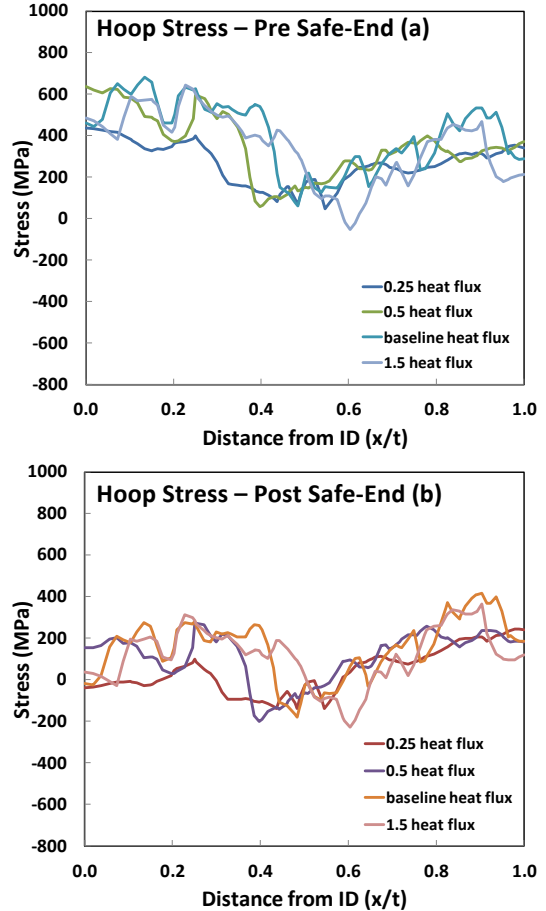

Figure 8 Hoop stress results for heat flux magnitude sensitivity study (a) pre- and (b) post-stainless steel safe-end weld.

The thermal heat flux model of [16] accounts for the weld speed for a given pass. By varying the weld speed, the duration of time over which the heat flux is applied changes; however the total energy applied, calculated as the integral of the heat flux with respect to time, remains the same. In the baseline analysis, the weld speed is approximately 2.54 mm/second, with minor variations for specific passes. To provide a wide range of heat flux durations in the sensitivity studies, the weld speeds of 0.75, 1.0, 1.75, 3.5, and 5.0 mm/sec are analyzed. Figure 9 shows the resulting heat flux magnitudes as a function of time, including the baseline case. Figures 10 and 11 show the final through-wall centerline DM weld axial and hoop stress distributions, before and after application of the stainless steel weld, for the various heat flux duration inputs. The magnitude of stress variation is significantly lower for the heat flux duration sensitivity study than for the heat flux magnitude sensitivity study.
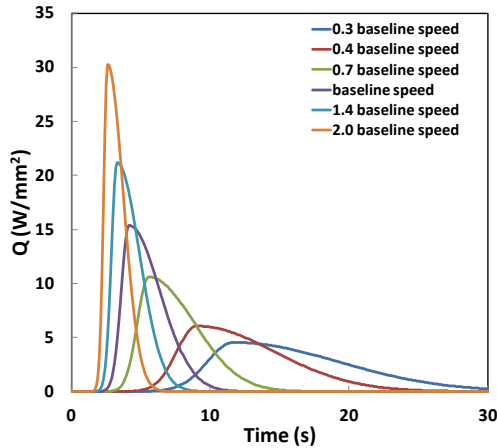
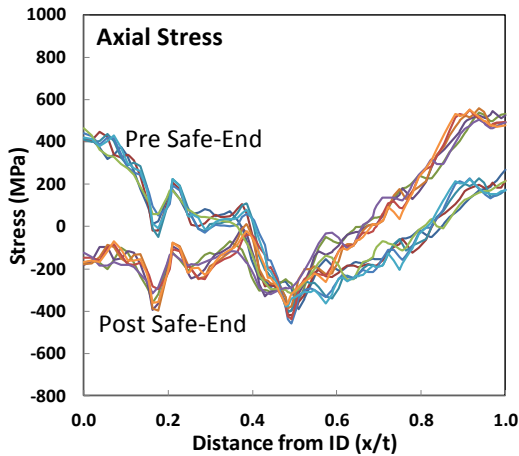**Figure 9** Heat flux vs. time for duration sensitivity study.

Figure 10 Axial stress results for heat flux duration sensitivity study.
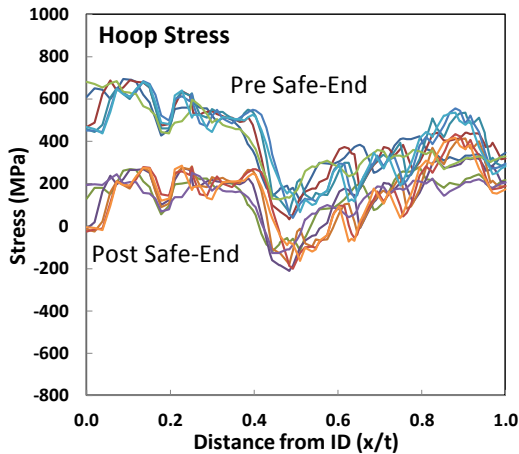

Figure 11 Hoop stress results for heat flux duration sensitivity study.

Plastic Properties (true stress vs true strain)

A sensitivity study is performed in which the elastic-plastic stress-strain response for the BE, Phase 2, and baseline properties are employed. Note that each of these material property sets are in the annealed condition. Figures 12 and 13 provide the axial and hoop stress results for these material properties. At the normalized through-wall distance of approximately 0.15, a significant difference between the baseline/BE properties and the Phase 2 properties. By process of elimination, it has been determined that the stainless steel pipe properties used in the baseline and BE studies cause this to occur; a comparison of these properties has not illuminated the source of this discrepancy and will need to be resolved in future work. Other than the difference at x/t=0.15, the remainder of the stress distributions are fairly consistent, with a moderate variation.
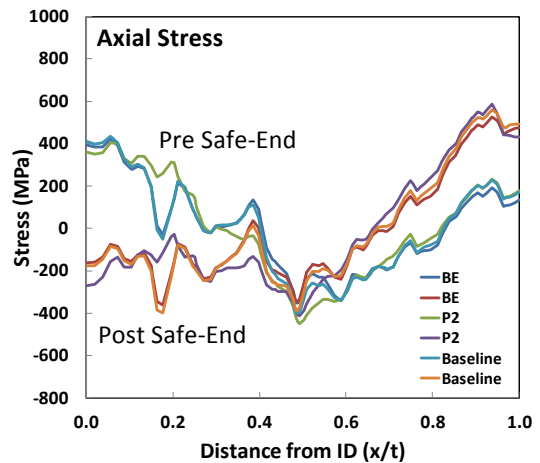

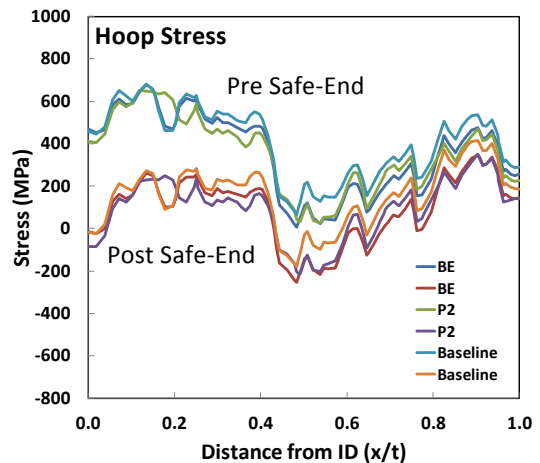**Figure 12** Axial stress results for material property sensitivity study.

Figure 13 Hoop stress results for material property sensitivity study.

Hardening Law (isotropic and kinematic)

A sensitivity study is performed in which the baseline material properties are used with linear kinematic and isotropic hardening laws. Note that only linear kinematic is studied; multi-linear kinematic and mixed isotropic/kinematic are not studied here. For consistency, the first and last data points in the original plastic stress-strain curves are retained in both the isotropic and linear kinematic hardening laws. Figures 14 and 15 provide the axial and hoop stress results for the hardening law sensitivity studies. Clearly, changing the hardening assumption from isotropic to linear kinematic results in quite a large variation in stress distribution.
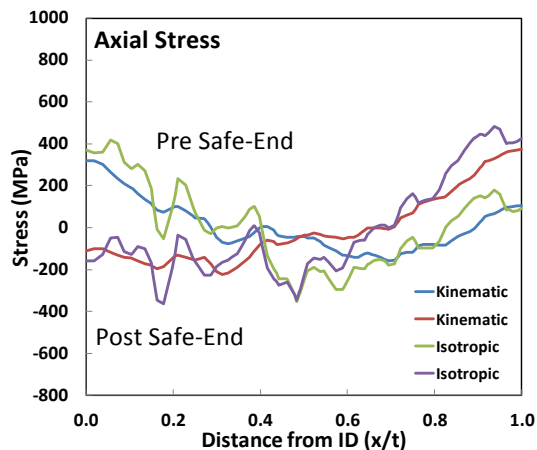

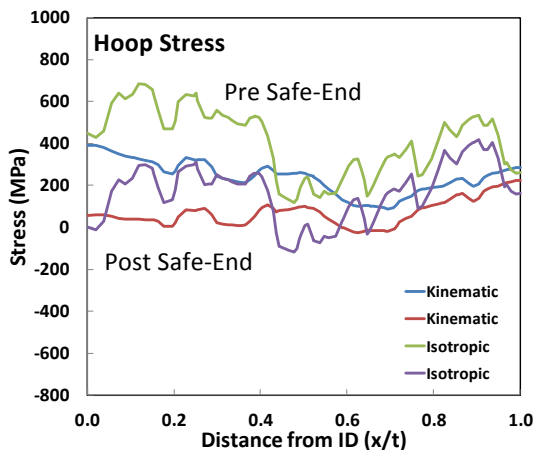**Figure 14** Axial stress results for hardening law sensitivity study.

Figure 15 Hoop stress results for hardening law sensitivity study.

DISCUSSION

There is clearly a significant amount of scatter in the calculated residual stress profiles. Although the average measurements and FE analysis results differ in places by significant stress levels, given the overall scatter in the results, they do occupy the same distribution. In reviewing input parameters provided by round robin participants, the stress results are highly sensitive to some parameters, and relatively insensitive to others. Of highest significance are the thermal energy input, post-yield stress-strain behavior, and treatment of strain hardening. The order of bead deposition, bead geometry and fabrication processes (such as the groove machining and re-weld procedure used in the current study) can play an important role in calculated stresses. The effect of the stainless steel weld on ID stresses has been demonstrated in this study. The sequence of DM weld, groove machining and re-weld used in the current study (and typical of how many nozzles were fabricated in the current fleet of operating reactors) demonstrates the evolution of stress fields through these fabrication steps.

There is no inherent reason why different FEA codes should provide different results. For example, preliminary sensitivity studies completed with the ANSYS [21] and ABAQUS [15] FEA codes have shown that the two codes are capable of providing effectively identical results. Early on in the investigation, it was felt that the treatment of annealing is fundamentally different in the two codes; however, the results indicate that, when properly applied by the analyst, the two codes provide consistent results. The results of these and other sensitivity studies will be presented in a future publication.

WRS assessment is an important step in flaw evaluation. The remaining steps in flaw evaluation include calculations of stress intensity factor (vs. through-wall thickness) and crack growth to assess fitness for service in terms of either allowable crack length or allowable stress. Future research will take the WRS results from the current study, and their associated variability, and perform flaw evaluation studies. From these calculations, the effect of variations in WRSs on flaw evaluations can be assessed [22].

SUMMARY

The U.S. NRC and EPRI are working cooperatively under an addendum to the ongoing memorandum of understanding to validate welding residual stress (WRS) predictions in pressurized water reactor (PWR) primary cooling loop components containing dissimilar metal (DM) welds. In this report, an international round robin analysis project is described in which participants analyzed a prototypic reactor coolant pressure boundary component. Mock-up fabrication, WRS measurements and comparison with predicted stresses through the DM weld region are described. Based on measured and calculated residual stress profiles, the mock-up fabricated in the current study has good correlation to known in-plant configurations.

The results of this study show that, on average, analysts can develop WRS predictions that are a reasonable estimate for actual configurations as quantified by measurements. However, the scatter in predicted results from analyst to analyst can be quite large. For example, in this study, the scatter in WRSs through the centerline of the main DM weld

(prior to stainless steel weld application) predicted by analysts is approximately +/- 200 MPa for axial and hoop stresses. Sensitivity studies assist in determining which input parameters provide significant impact on WRSs, and those that do not. It is shown that thermal energy input, post-yield stress-strain behavior, and treatment of strain hardening have the greatest impact on DM WRS distributions.

ACKNOWLEDGMENTS

REFERENCES

1. The Shim, D. J., Kalyanam, S., Punch, E., Zhang, T., Brust, F.W., Wilkowski, G., Goodfellow, A. and Smith, M., "Advanced Finite Element Analysis (AFEA) Evaluation for Circumferential and Axial PWSCC Defects", Proceedings of the 2010 ASME Pressure Vessels Piping conference, Seattle, WA, PVP2010-25162.
2. Rudland, D., Zhang, T., Wilkowski, G., Csontos, A., 2008 "Welding Residual Stress Solutions for Dissimilar Metal Surge Line Nozzles Welds," Proceedings of the 2008 ASME Pressure Vessels Piping conference, Chicago, IL, PVP2008-61285.
3. Rathbun, H.J., Fredette, L.F., Scott, P.M., Csontos, A.A., Rudland, D.L., "NRC Welding Residual Stress Validation Program International Round Robin Program and Findings," Proceedings of the 2011 ASME Pressure Vessels and Piping Conference, Baltimore, MD, PVP2011-57642.
4. Fredette, L.F., Kerr, M., Rathbun, H.J., Broussard, J.E., "NRC/EPRI Welding Residual Stress Validation Program - Phase III Details and Findings," Proceedings of the 2011 ASME Pressure Vessels and Piping Conference, Baltimore, MD, PVP2011-57645.
5. Zhang, T, Brust, F., W., Wilkowski, G., 2011 "Weld Residual Stress in Large Diameter Nuclear Nozzles," Proceedings of the 2011 ASME Pressure Vessel Piping conference, Baltimore, MD, PVP2011-57959.
6. Addendum to the Memorandum of Understanding (MOU) between NRC's Office of Nuclear Regulatory Research and Electric Power Research Institute, Inc. on Cooperative Nuclear Safety Research", NRC ADAMS Accession Number ML103490002.
7. Rudland, D., Kurth, R., Bishop, B., Mattie, P., Klasky, H., Harris, D., 2010 "Development of Computational Framework and Architecture for Extremely Low Probability of Rupture (XLPR) Code," Proceedings of the 2010 ASME Pressure Vessel Piping conference, Seattle, WA, PVP2010-25963.
8. US Nuclear Regulatory Commission, Office of Nuclear Regulatory Research, Division of Engineering, Component Integrity Branch: International Weld Residual Stress Round Robin Problem Statement.
9. Rudland, D., Csontos, A., Brust, F., Zhang, T., 2009, "Welding Residual Stress and Flaw Evaluation for Dissimilar Metal Welds with Alloy 52 Inlays," Proceedings of the 2009 ASME Pressure Vessel Piping conference, Prague, Czech Republic, PVP2009-77167.
10. Kingston, E. J., Stefanescu, D., Mahmoudi, A. H., Truman, C. E., and Smith, D. J., "Novel Applications of the Deep-Hole Drilling Technique for Measuring Though-Thickness Residual Stress Distributions," Journal of ASTM International, 2006, Vol. 3, No. 4.
11. Mahmoudi, A-H., Smith, D., J., Truman, C., E., Pavier, M., J., 2009, "Application of the Modified Deep Hole Drilling Technique (iDHD) for Measuring Near Yield Non-Axisymmetric Residual Stresses," Proceedings of the ASME 2009 Pressure Vessels & Piping Division Conference, Prague, Czech Republic, PVP2009-77940.
12. DeWald, A.T., Hill, M.R., Willis, E., "Measurement of Welding Residual Stress in Dissimilar Metal Welds Using the Contour Method," Proceedings of the ASME 2011 Pressure Vessels & Piping Division Conference, Baltimore, MD, PVP2011-57720.
13. Wang, X-L., Feng, Z., Spooner, S. Hubbard, C. R., and Taljat, B. "Characterization of Welding Residual Stresses with Neutron Diffraction," Proceedings of the 1998 Taiwan Intentional Welding Conference.
14. Noyan, I.C., Cohen J.B., Residual Stress Measurement by Diffraction and Interpretation, New York, Springer-Verlag, 1987.

15. ABAQUS User Manual, Simulia, Dassault Systems, version 6.10, 2010.
16. Goldak, J., Chakravarti, A., Bibby, M., "A New Finite Element Model for Welding Heat Sources," Metallurgical Transactions, 1984, Vol. 15B.
17. Feng, Z., Wolfe, K., Willis, E. "A Computational Modeling Tool for Welding Repair of Irradiated Materials," 19th International Conference on Nuclear Engineering, 2011, Chiba, Japan, ICONE19-44103.
18. Taljat, B., Zacharia, T., Wang, X-L, Keiser, J.R., Swinderman, R.W., Feng, Z., and Jirinec, M.J., "Numerical Analysis of Residual Stress Distribution in Tubes with Spiral Weld Overlay," Welding Journal, 1998, Vol. 77, No. 8.
19. Feng, Z., "A Computational Analysis of Thermal and Mechanical Conditions for Weld Metal Solidification Cracking," Welding in the World, 1994, Vol. 33, No. 5.
20. Brust, F.W., Zhang, T., Shim, D-J, Kalyanam, S., Wilkowski, G., Smith, M., Goodfellow, A., "Summary of Weld Residual Stress Analyses for Dissimilar Metal Weld Nozzles," Proceedings of the 2010 ASME Pressure Vessels and Piping conference, Seattle, WA, Paper PVP2010-25162.
21. ANSYS Finite Element Computer Code, Version 12.1, ANSYS, Inc., Canonsburg, PA.
22. DJ Shim, M Kerr, S Xu, "Effect of Weld Residual Stress Fitting on Stress Intensity Factor for Circumferential Surface Cracks in Pipe," Proceedings of the 2012 ASME Pressure Vessels and Piping conference, Toronto, ON, Canada, Paper2012-78180.